Role of the Tibetan Plateau on the Annual Variation of Mean Atmospheric Circulation and Storm-Track Activity*

SUN-SEON LEE,[+] JUNE-YI LEE,[#] KYUNG-JA HA,[+] BIN WANG,[#] AKIO KITOH,[@] YOSHIYUKI KAJIKAWA,[&] AND MANABU ABE**

[+] *Division of Earth Environmental System, Pusan National University, Busan, South Korea*
[#] *International Pacific Research Center, and Department of Meteorology, University of Hawaii, Honolulu, Hawaii*
[@] *Meteorological Research Institute, Tsukuba, Japan*
[&] *Advanced Institute for Computational Science, RIKEN, Kobe, Japan*
** *Arctic Environment Research Center, National Institute of Polar Research, Tokyo, Japan*

(Manuscript received 30 March 2012, in final form 18 January 2013)

ABSTRACT

This study reexamines how the Tibetan Plateau (TP) modulates the annual variation of atmospheric circulation and storm-track activity based on the Meteorological Research Institute's atmosphere–ocean coupled model experiments with a progressive TP uplift from 0% to 100% of the present height. Three major roles of the TP on atmospheric circulation and storm-track activity are identified. First, consistent with a previous finding, the TP tends to intensify the upper-level jet and enhance baroclinicity in the North Pacific Ocean but significantly weaken storm-track activity over the TP, East Asia, and the western North Pacific during the cold season. Second, the TP amplifies stationary waves that are closely linked to transient eddies. In particular, the TP enhances the Siberian high and the Aleutian low, which together contribute to the strengthening of the East Asian winter monsoon circulation and the weakening of storm-track activity. Third, the TP significantly modulates the subseasonal variability of the Pacific storm-track (PST) activity. In particular, the TP tends to suppress PST activity during midwinter despite the fact that it strengthens baroclinicity along the Pacific jet. The midwinter suppression of PST activity, which is well reproduced in a control run with a realistic TP, gradually disappears as the TP height decreases. Major factors for the midwinter suppression of the PST associated with the TP include the 1) destructive effect of an excessively strong jet leading to an inefficiency of barotropic energy conversion, 2) reduction of baroclinicity over the northern part of the TP, and 3) subseasonally varying SST change and resulting moist static energy.

1. Introduction

Large topographic features such as the Tibetan Plateau (TP) and the Rocky Mountains exert significant impacts on weather and global climate. The TP is one of the major topographic features in the world. Many previous studies examined the mechanical and thermodynamical effects of the TP on the variability of global climates (Liu et al. 2012; Wu et al. 2012a,b). It is noted that the thermal forcing by the TP on the Asian monsoon climate exhibits a weakening trend (Liu et al. 2012). Unlike summer, when the thermal forcing of the TP is dominant, the mechanical effect of the TP becomes more important than the thermal effect in winter. The retarding and deflecting effects of the TP as a large obstacle generate an asymmetric dipole structure of wind with an anticyclone to the north and a cyclone to the south of the TP (Wu et al. 2007). The northward deflection of the westerly flow along the northern TP and the resulting enhancement of the meridional temperature gradient contribute to a favorable condition for the growth of baroclinic eddies (Saulière et al. 2012). Broccoli and Manabe (1992) noted that large-amplitude stationary waves develop owing to the presence of the TP and these waves influence the midlatitude climate.

In addition to such important factors as background flow, land–sea contrast, and diabatic heating, topography

* School of Ocean and Earth Science and Technology Publication Number 8824 and International Pacific Research Center Publication Number 943.

Corresponding author address: Dr. June-Yi Lee, University of Hawaii/International Pacific Research Center, POST Bldg., Room 403B, 1680 East West Road, Honolulu, HI 96822.
E-mail: juneyi@hawaii.edu

DOI: 10.1175/JCLI-D-12-00213.1

also affects storm-track activity. Using a simple dry balance model, Lee and Mak (1996) examined the role of Northern Hemisphere (NH) orography in the maintenance of storm tracks in winter. They suggested that zonal flow interacting with orography could reinforce the localized baroclinicity in the western part of the Pacific and the Atlantic Oceans. Son et al. (2009) discussed that a prominent topographic feature modifies the downstream storm-track intensity and such an effect is highly dependent on the structure of the background flow. In regard to the subseasonal variability of storm-track activity, it was suggested that the midwinter suppression of the Pacific storm-track (PST) activity is caused by a midwinter minimum Eady growth rate over midlatitude Asia (Penny et al. 2010). Park et al. (2010) showed that a decrease in storm-track activity is associated with a weakening of downstream eddy development and a suppression of baroclinic energy conversion over eastern Eurasia in the presence of the central Asian mountains.

While recent research has pointed out a potential importance of stationary waves and the associated eddy-seeding effect on North Pacific transient eddies (Penny et al. 2010; Park et al. 2010), dynamical linkage between stationary waves and transient eddies is still not well understood. Effects of topography-forced stationary waves on downstream transient eddy activity should be examined further to better understand the storm-track dynamics. In this study, the effects of orography on the seasonal mean, subseasonal variability, and the annual cycle of the mean flow and transient eddy activity are explored in depth based on a TP height control experiment with an atmosphere–ocean GCM (AOGCM). In particular, the role of the TP on the midwinter suppression of the PST is focused.

Section 2 describes the model and the experimental design. In section 3, changes in the time-mean flow by TP-induced stationary waves during the cold season are discussed. In particular, upper- and low-level circulations, surface pressure systems, and temperature changes are compared. Section 4 is devoted to an examination of the impact of TP on the subseasonal variability of storm-track activity. Possible factors controlling the subseasonal variability of PST activity are discussed in section 5. Specifically, jet intensity, barotropic energetics, baroclinicity, and sea surface temperature (SST) effects are investigated. A summary and discussion follow in section 6.

2. Model and experiment

A numerical model used in this study is the Meteorological Research Institute (MRI) Coupled Atmosphere–Ocean General Circulation Model, version 2.3.2 (MRI-CGCM 2.3.2; Yukimoto et al. 2001, 2006). The atmospheric component of the model has a T42 resolution (about 2.8° × 2.8°) and 30 vertical levels with the top at 0.4 hPa. The distribution of vegetation types is fixed. The oceanic component of the model is a Bryan–Cox-type ocean GCM (OGCM). The OGCM has a 2.5° × 2° longitude–latitude resolution and 23 vertical layers. Near the equator, between 4°S and 4°N, the latitudinal grid spacing is set to 0.5° in order to maintain a good resolution for the equatorial oceanic waves. The atmosphere–ocean coupling interval is 24 h and a flux adjustment was performed at the interface.

To examine the role of the TP on the time-mean flow and transient eddy activity, five different TP heights were used: 0% (TP00), 25% (TP25), 50% (TP50), 75% (TP75), and 100% (TP100, control run). The TP100 experiment has a realistic TP height. The TP height is zero in the TP00 experiment. In all model integrations, the land–sea configurations as well as the initial conditions are the same. Except for the TP, a realistic orography was used, which differs from Abe et al. (2003, 2004) and Kitoh (2004, 2007); the latter studies show the effect of global mountain changes using the MRI-CGCM, versions 1 and 2. In addition, MRI-CGCM 2.3.2 has more realistic mean fields of SST, precipitation, and circulation with realistic global mountains (not shown) than the older versions used in previous studies. Thus, it is anticipated that the new version provides a more reliable estimation of the role of the TP on storm-track activity than the older ones since the correction of inherent bias in the mean state of a model is critical for improving simulations of variability (Lee et al. 2010). All runs are executed for 50 years and the last 35-yr data are used for the analysis in this study. Figure 1 shows the TP height condition in five experiments used in this study.

3. Changes in seasonal-mean structure

First, the effect of topography in controlling the position and amplitude of the jet stream is examined since storm-track activity is closely related to the background flow. Figure 2 presents the 300-hPa zonal wind averaged over the cold season [November–March (NDJFM)] from the National Centers for Environmental Prediction (NCEP)/U.S. Department of Energy (DOE) Atmospheric Model Intercomparison Project (AMIP)-II reanalysis (Reanalysis-2; Kanamitsu et al. 2002) and the five experiments. The 500- and 850-hPa zonal winds averaged over the latitude band 35°–40°N are also given in Figs. 2g and 2h; the cores of the Pacific and the Atlantic jet streams are located in this latitude band. As the TP height increases, with an exception of TP00,

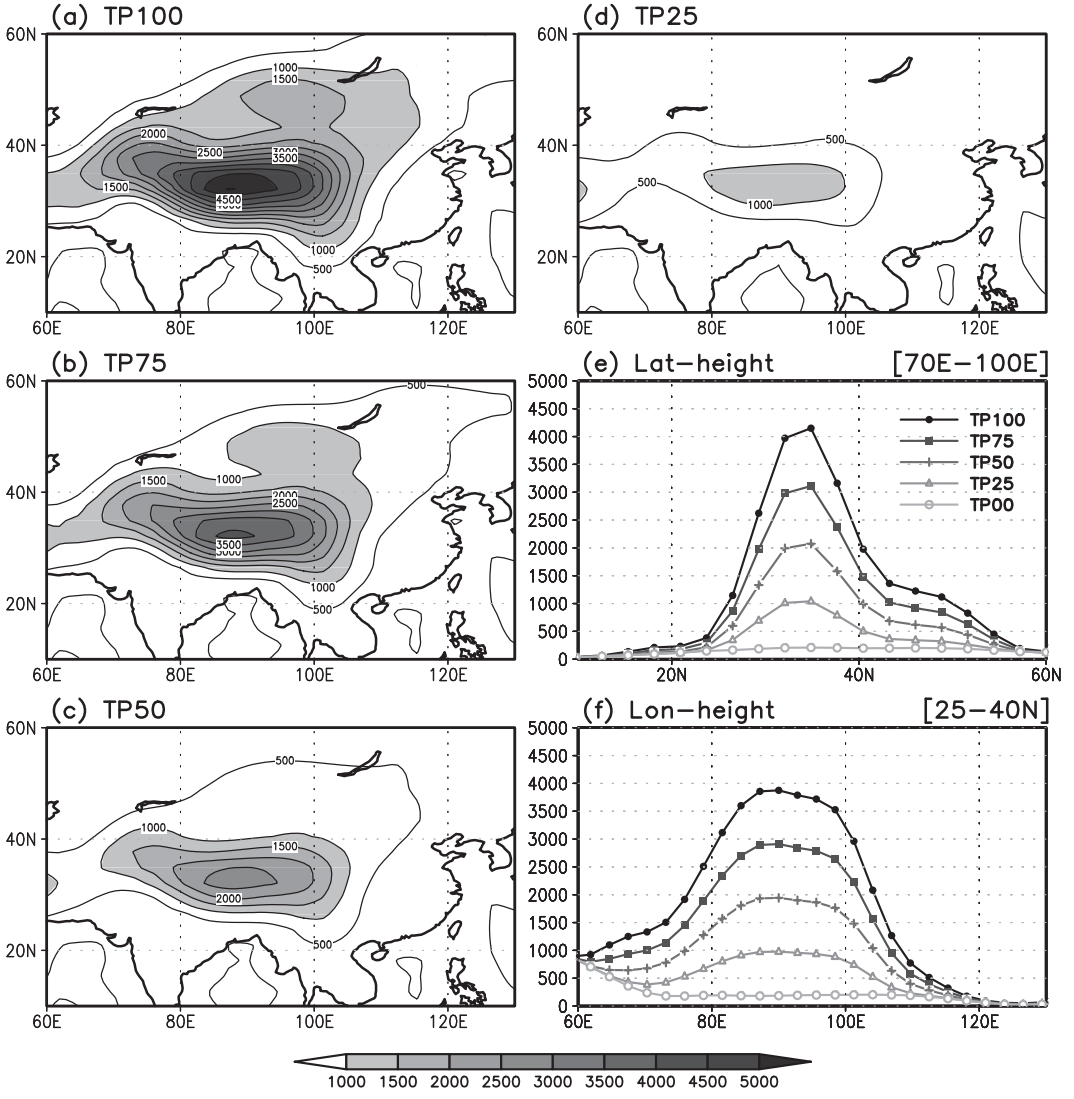

FIG. 1. (a)–(d) Maps of the topography for the TP simulations (m, MSL). (e),(f) Lat–height and lon–height, respectively. Here, TP100 indicates that the ratio of TP height in the experiment to that of the real TP is 1.0 (100%) and so forth.

the upper-tropospheric Pacific jet core intensity during the cold season increases while the zonal wind over the TP weakens. A similar feature is also found in Figs. 2g and 2h. The TP00 experiment yields a result that is slightly inconsistent with other experiments; while the zonal wind over the TP is weaker, the Pacific jet core is stronger than TP25 (Figs. 2f–h). The Pacific jet core during the cold season in TP00 is stronger than its counterpart in TP25 because of a stronger jet in December and January (not shown).

Compared with Reanalysis-2, the core of the Pacific jet is shifted slightly eastward to approximately 160°E in all the experiments. The latitudinal location of the Pacific jet core, however, is not affected by the TP. It is noted that the southward shift of the Pacific jet as it passes the TP becomes more pronounced with the increase of the TP elevation. Meanwhile, the Atlantic jet exhibits no clear tendency with the TP height, implying that the Atlantic jet is not significantly influenced by the TP. The southwest–northeast tilt of the Atlantic jet in Reanalysis-2 is much less in all the experiments. Figures 2g and 2h indicate that the TP effect on the jet stream is large to the west of the date line. In particular, the zonal wind difference between TP75 and TP50 is outstanding at approximately 160°E.

Since transient eddy activity is strongly linked with stationary waves (e.g., Branstator 1992; Chang 2009), the characteristics of the stationary eddy component

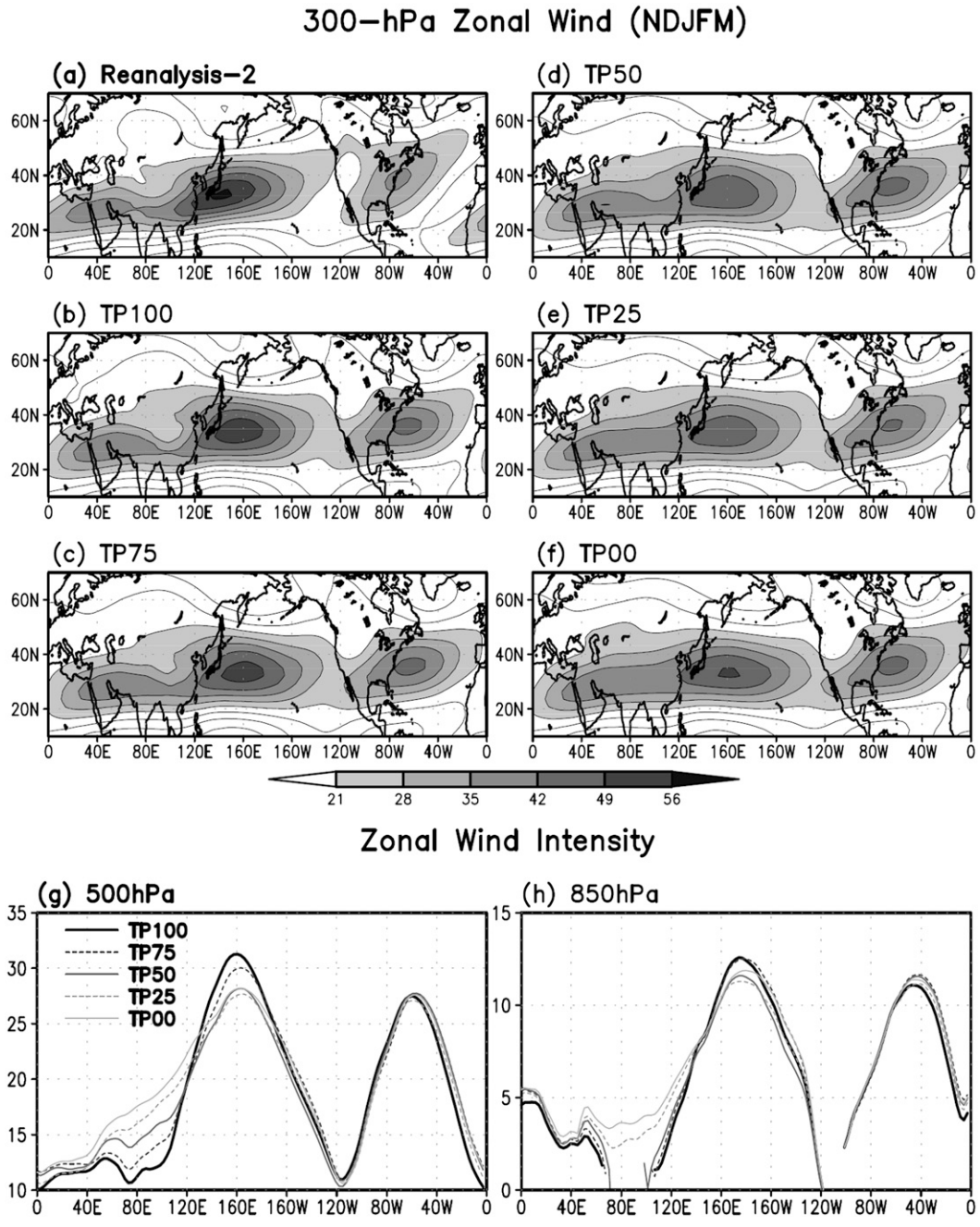

FIG. 2. The averaged 300-hPa zonal wind (m s^{-1}) during NDJFM obtained from (a) Reanalysis-2, (b) TP100, (c) TP75, (d) TP50, (e) TP25, and (f) TP00. The zonal wind intensities at (g) 500 and (h) 850 hPa are averaged over the latitude band 35°–40°N.

(deviation from the zonal mean) in the surface pressure system are examined in Reanalysis-2 and the TP experiments (Fig. 3). The dominant features in the surface pressure system in winter are the Siberian high and the Aleutian low, which together control the structure and variability of the East Asian winter monsoon (EAWM) system (Wang et al. 2010; Lee et al. 2013). Nakamura et al. (2002) showed that the weakening of the Siberian high and the EAWM is related to the midwinter weakening of the PST. The Siberian high over the Asian continent and the Aleutian low over the North Pacific are faithfully reproduced by MRI-CGCM 2.3.2 (Fig. 3b). It is noted that both the Siberian high and the Aleutian low are enhanced with the height of the TP, while their center

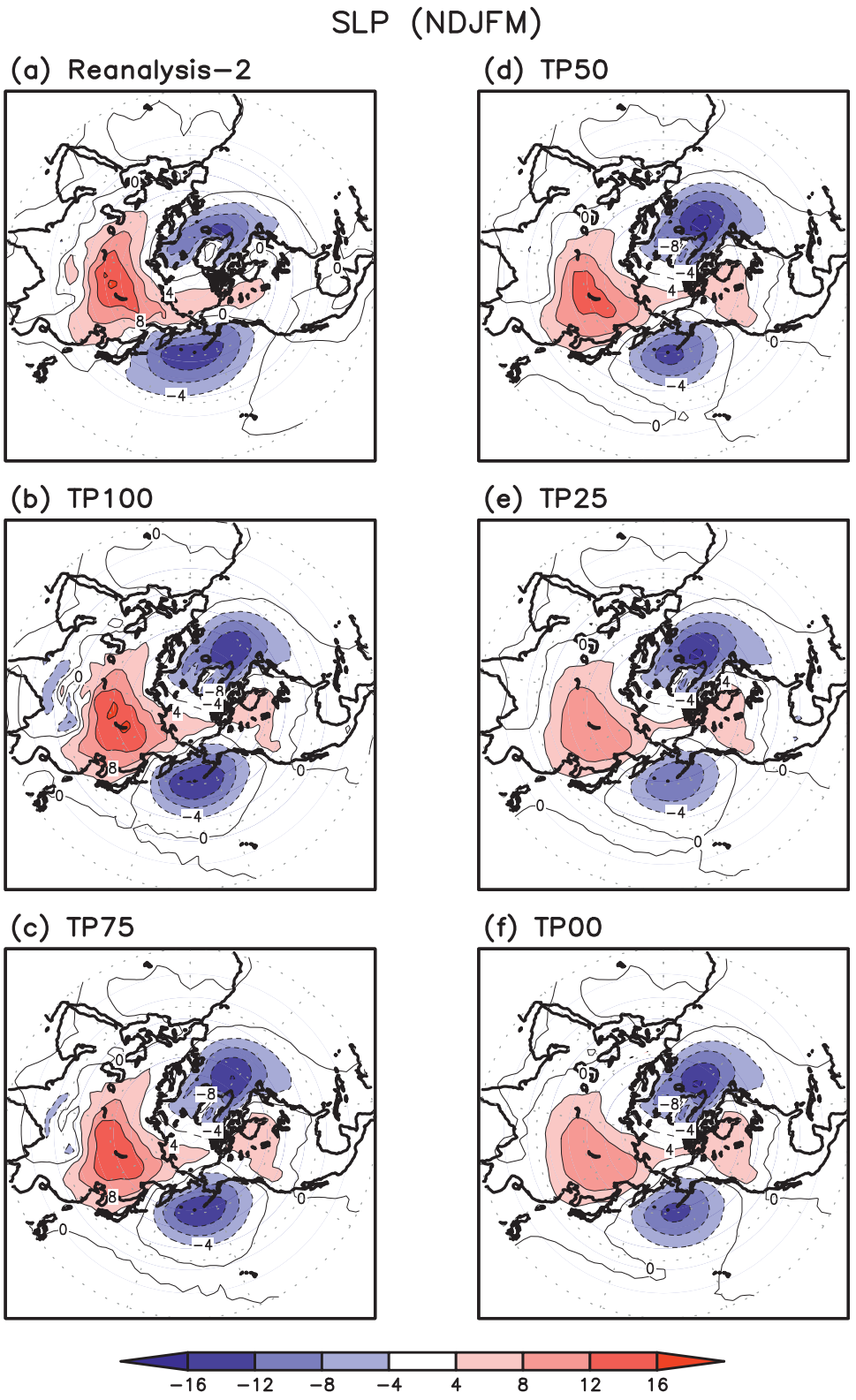

FIG. 3. The stationary eddy component (departure from the zonal mean; hPa) of SLP during NDJFM obtained from the (a) Reanalysis-2, (b) TP100, (c) TP75, (d) TP50, (e) TP25, and (f) TP00 experiments.

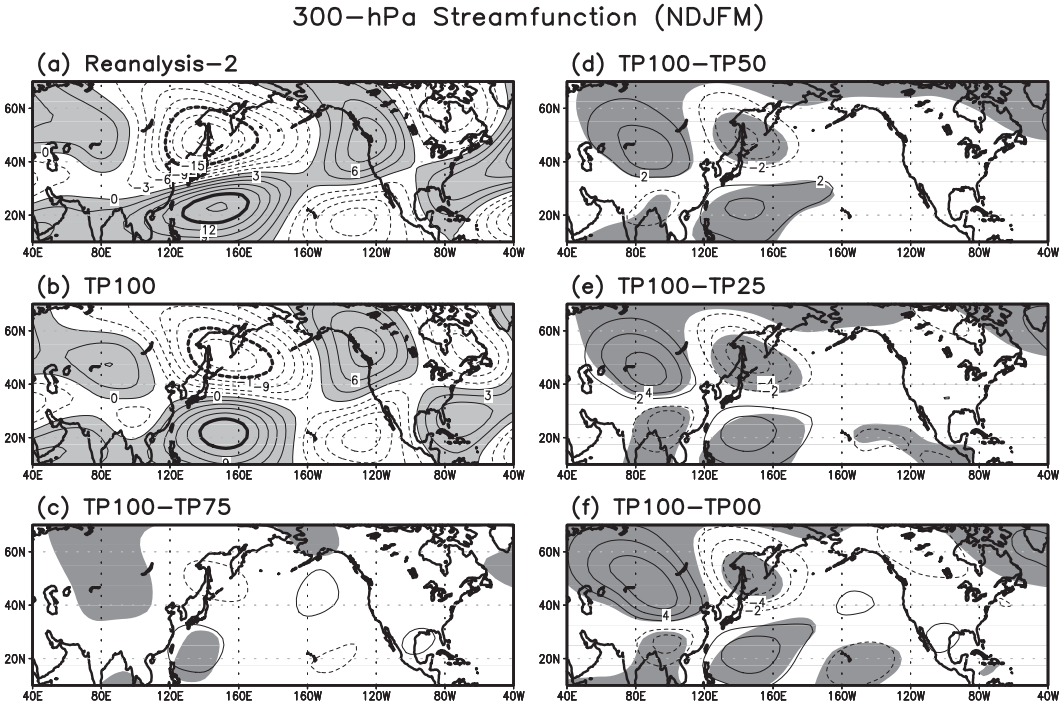

FIG. 4. The 300-hPa streamfunction of stationary waves (departure from the zonal mean; 10^6 m^2 s^{-1}) averaged over NDJFM derived from (a) Reanalysis-2 and (b) TP100. The differences of the 300-hPa streamfunction averaged over NDJFM between (c) TP100 and TP75, (d) TP100 and TP50, (e) TP100 and TP25, and (f) TP100 and TP00. Thick contours in (a),(b) correspond to 15×10^6 m^2 s^{-1} (solid contour) and -15×10^6 m^2 s^{-1} (dashed contour). Shading in (c)–(f) denotes a 95% confidence level.

positions remain nearly the same in all the experiments. This is in accordance with Kitoh (2002), who showed that both the Siberian high and the Aleutian low are more intense in a present-day orography experiment than in a no-mountain experiment. The similarity of the sea level pressure (SLP) changes in the TP experiment and the global mountain experiment indicates that the TP alone can exert a significant influence on the NH atmospheric circulation by intensifying the Siberian high and the Aleutian low. As in Fig. 2, the Aleutian low, downstream of the TP, becomes slightly stronger in TP00 than in TP25, while the magnitude of the Siberian high remains the same in the two experiments.

Although orographic forcing generates weaker winter stationary waves than does the diabatic heating (Held et al. 2002; Chang 2009), the former plays an important role in the development of transient eddies. To examine the effect of the TP on the stationary waves, the 300-hPa streamfunction in the NH is calculated (Fig. 4). The simulated stationary wave pattern in TP100 is comparable to the observed counterpart except for a slight northeastward shift of a weaker negative core over the western North Pacific (Figs. 4a and 4b). A comparison between TP100 and other experiments reveals that substantial differences are found over the TP region and the western North Pacific, which indicates that the TP plays a significant role in amplifying stationary waves over the TP and its downstream region, that is, the western North Pacific. However, the amplitude change of the stationary waves with the TP height in January (not shown) and the cold season, in general, in the MRI-CGCM is smaller than that in Park et al. (2010, 2011) and Chang and Lin (2011). Difference in the physics and dynamics of the models causes somewhat different sensitivities of stationary waves to the TP elevation. In addition, Fig. 4 suggests that the TP should not influence in any substantial way stationary waves over North America, contrary to the result of Held et al. (2002). This discrepancy may also be related to the physical and dynamical differences of the models and indicate that our understanding of how orography affects stationary waves is still insufficient.

We further examine the TP effect on the EAWM by comparing circulation and temperature in the TP100 and TP25 experiments. Figures 5a and 5b show the low-level wind and surface temperature during December–January (DJ) in TP100 and TP25, respectively. While the northwesterly wind over the northeastern part of the

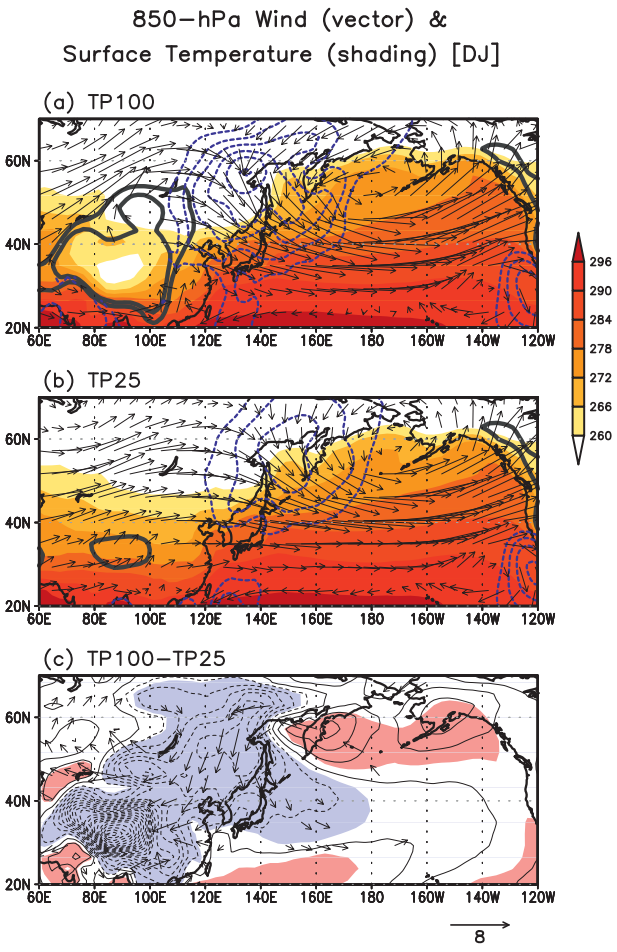

FIG. 5. The 850-hPa wind [vector, reference vector below (c); m s^{-1}], 850-hPa northerly wind (blue dotted contour; interval 1 m s^{-1}), and surface temperature (shading; K) averaged over DJ in the (a) TP100 and (b) TP25 experiments. (c) Difference in 850-hPa wind (vector) and surface temperature (contour; interval 1 K) averaged over DJ between TP100 and TP25. Gray contours in (a),(b) indicate mountains and the contour levels are 1000 and 1500 m. Shading in (c) denotes that surface temperature difference is significant at a 95% confidence level. Wind vectors significant at a 95% confidence level are shown in (c).

Asian continent, a crucial component of the EAWM, is prominent in the TP100 experiment, the zonal flow pattern dominates the circulation field over northeast Asia including China, the Korean Peninsula, and Japan in the TP25 experiment. In particular, the northerly wind (blue dotted contours in Fig. 5a) extends farther to the south of the Korean Peninsula and Japan in the TP100 experiment. The northerly flow in TP25, on the other hand, is confined to the north of the Korean Peninsula and the Sea of Okhotsk. The northerly anomaly, henceforth, is a distinct difference between TP100 and TP25 (Fig. 5c). The anomalous cold advection by stronger northerly wind is responsible for a stronger EAWM and vice versa. A negative temperature anomaly is dominant not only over the TP, but also over East Asia in the TP100-minus-TP25 difference as a result of the northerly anomaly. Meanwhile, the warm temperature anomaly over the Sea of Okhotsk seems related to a stronger southeasterly or easterly wind associated with a deeper Aleutian low over the North Pacific in TP100 relative to TP25 as shown in Fig. 3. The strengthening of the EAWM and the Siberian high in the presence of the TP leads to an intensification of the midwinter minimum of the PST. This issue will be revisited in section 5.

The results presented in Figs. 6a and 6b also show a clear dependence of circulation over East Asia on the elevation of the TP. In the annual cycles of zonal and meridional winds over the region (30°–50°N, 105°–145°E), TP100-minus-TP25 difference is larger in winter than in summer. This implies that the TP exerts stronger influence on the East Asian circulation over the region (30°–50°N, 105°–145°E) during winter than summer in MRI-CGCM 2.3.2. The zonal wind becomes stronger, particularly in winter, when the TP height decreases, indicating that a high-topographic feature weakens the downstream zonal wind. In a realistic TP condition, there is a stronger northerly wind in winter and a stronger southerly wind in summer than in other simulations. The seasonal variation of the meridional wind is clearly seen even when the TP altitude is zero.

4. Changes in storm-track activity

a. NDJFM-mean change

In this section, we examine changes in transient synoptic eddy activity by the presence of the TP during the entire cold season. In the present study, storm-track activity is defined in terms of the root-mean-square (RMS) values of 2–8-day bandpass-filtered meridional wind at 300 hPa. Figure 7 shows the observed and simulated storm-track activity during NDJFM. The coupled model with a realistic TP (Fig. 7b) is capable of simulating the observed features of the climatological storm-track activities, particularly over Asia and the Pacific. On the other hand, the model tends to underestimate the Atlantic storm-track (AST) activity. In the observations, the PST is weaker than the AST during the entire cold season (e.g., Lee et al. 2011, 2012b). Figures 7c–f show that storm-track activity tends to weaken over the TP area, East Asia, and the western North Pacific during the cold season as the TP height increases. The location of the maximum PST activity is not affected by the TP height.

b. Subseasonal variation

In the annual cycle, PST activity exhibits double peaks in late fall and early spring, but the AST activity shows

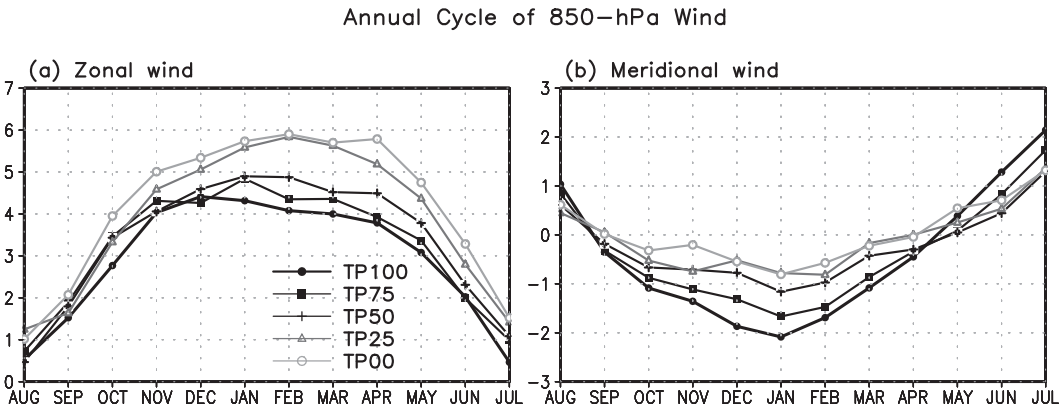

FIG. 6. The annual cycle of 850-hPa (a) zonal and (b) meridional wind (m s^{-1}) over the region (30°–50°N, 105°–145°E).

a single peak in midwinter (e.g., Nakamura 1992; Lee et al. 2011). Since the TP effect on the jet stream and storm-track activity is larger over the North Pacific than over the North Atlantic, the subseasonal variability of PST activity is focused (Fig. 8). The MRI-CGCM is capable of reproducing the double peaks and the midwinter minimum in the annual cycle of PST activity with a realistic TP as shown in Fig. 8a, although the midwinter suppression of PST activity is slightly underestimated compared to Reanalysis-2. It is noted that the TP plays a crucial role on the subseasonal variation of PST activity. The midwinter suppression of PST activity diminishes as the TP height decreases and subsequently TP25 exhibits a single peak in midwinter. The midwinter suppression of PST activity, however, appears again in TP00. This may be related to a stronger Pacific jet in TP00 than in TP25 as shown in Fig. 2; an excessively strong jet hinders baroclinic eddy growth (Nakamura

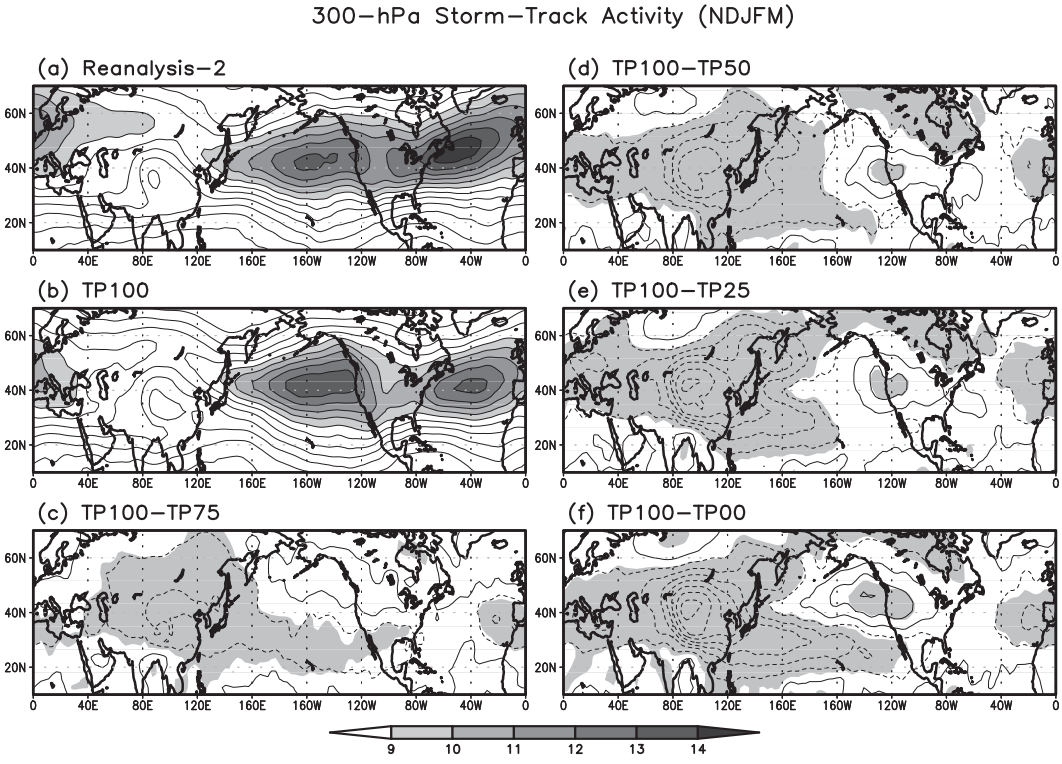

FIG. 7. The 300-hPa storm-track activity (m s^{-1}) averaged over NDJFM derived from (a) Reanalysis-2 and (b) TP100. The difference of the storm-track activity averaged over NDJFM between (c) TP100 and TP75, (d) TP100 and TP50, (e) TP100 and TP25, and (f) TP100 and TP00. Shading in (c)–(f) denotes that the values are significant at a 95% confidence level.

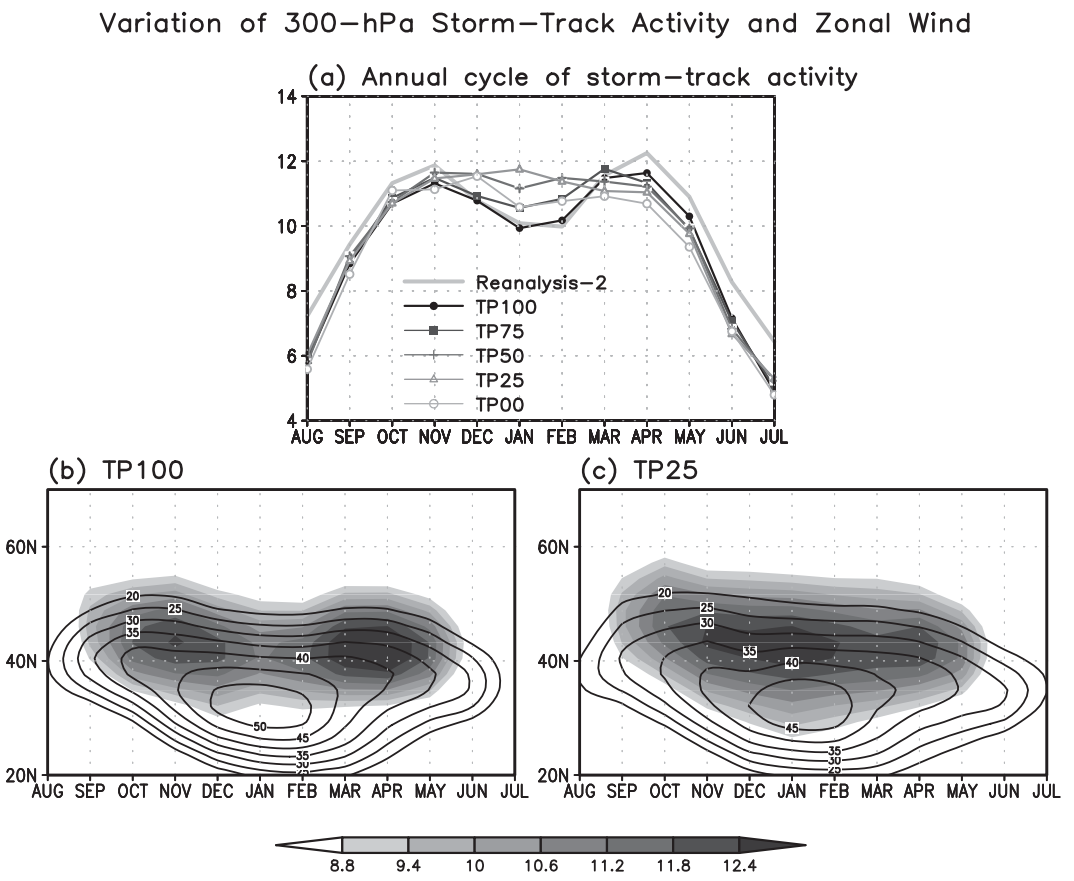

FIG. 8. The annual cycle of (a) 300-hPa storm-track activity (m s^{-1}) over (35°–55°N, 140°E–140°W) in Reanalysis-2 and the TP experiments. The time–latitude cross section of the 300-hPa storm-track activity (shading) and zonal wind (contour; m s^{-1}) are shown for (b) TP100 and (c) TP25. Storm-track activity was averaged over 140°E–140°W and zonal wind was averaged over 120°E–170°W in (b),(c).

1992). Interestingly, TP00 shows a stronger peak in December.

The time–latitude cross section of the 300-hPa PST activity and zonal wind further illustrates a distinct difference between TP100 and TP25 (Figs. 8b and 8c). TP100 shows double peaks of PST activity along with a stronger Pacific jet than TP25. The peak in March is stronger than that in November. Observations also show similar characteristics (Fig. 2a in Lee et al. 2011). Figure 9 further shows transitions of the PST and the jet from November to March in TP100 and TP25. It is noted that both experiments simulate a southward shift of the Pacific jet and the PST during midwinter. Although the latitudinal movement of the jet from November to March is similar in both the experiments, change in PST activity is considerably different between the two.

5. Factors for the midwinter minimum of the PST

This section describes how the TP affects the midwinter minimum PST activity by comparing TP100 with TP25. We identify three major factors for the midwinter PST minimum induced by the TP.

a. Changes in the jet, eddy structure, and local energetics

It is found that the TP modulation of the seasonal variation of the Pacific jet along with eddy structure and local energetics contribute to the midwinter suppression. Figure 9 indicates that the TP tends to intensify the Pacific jet in January resulting in a weakening of PST activity, despite a strong baroclinicity over the North Pacific. Similar to the hindering effect of an excessively strong jet in Nakamura (1992), storm-track activity tends to intensify linearly as the Pacific jet increases up to about 40 m s^{-1} but weakens after that in the experiments (Fig. 10). When the jet intensity is stronger than 40 m s^{-1}, a negative correlation of −0.36 is found between the jet speed and the PST activity in January in TP100, and the negative relationship becomes either weak in January (correlation = −0.18) or positive in March (correlation = 0.13) in TP25. Figure 10 also suggests

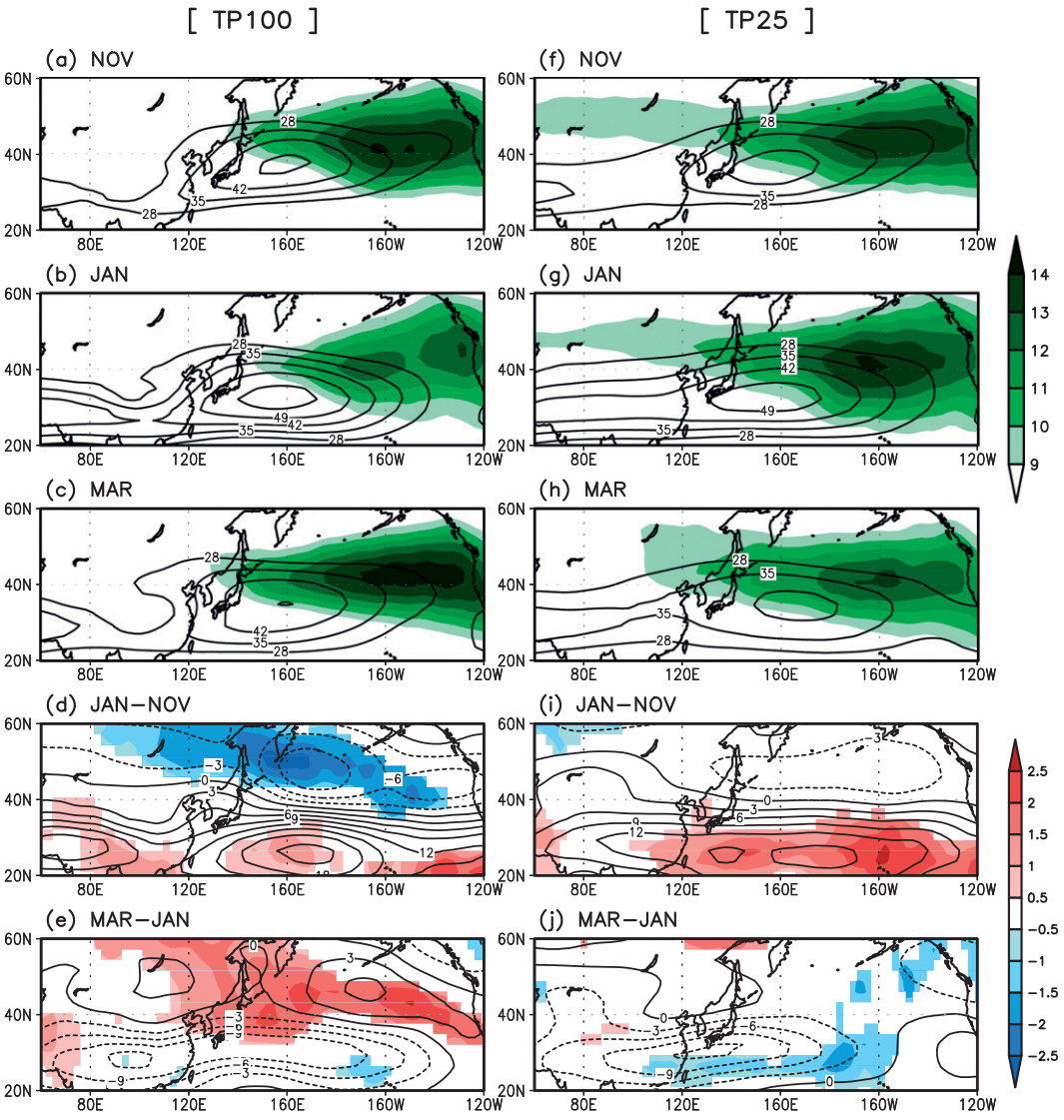

FIG. 9. The 300-hPa storm-track activity (shading; m s^{-1}) and zonal wind (contour; m s^{-1}) in (left) TP100 and (right) TP25 for (a),(f) November; (b),(g) January; (c),(h) March; (d),(i) difference between January and November; and (e),(j) difference between March and January. Shading in (d),(e),(i),(j) signifies that the differences are significant at a 95% confidence level. The top color scale refers to shading in (a)–(c) and (f)–(h).

that a narrower range of the amplitude variation of the Pacific jet in TP25 is more favorable for the PST intensification than a wider range in TP100.

The destructive effect of the excessively strong jet is related to an inefficient barotropic energy conversion from the mean flow to eddies in TP100. Lee et al. (2011) demonstrated that barotropic energy conversion associated with a shearing deformation of the background flow is essential for a PST initiation. Although the jet is stronger in TP100 than in TP25, barotropic energy conversion from the mean flow to transient eddies (positive) is much weaker, particularly during January (Fig. 11). This indicates that the barotropic governor effect, which is associated with meridional shear (James 1987), is strong during midwinter in TP100. The strong barotropic governor effect may contribute to the inefficiency of barotropic energy conversion. On the other hand, Chen et al. (2007) addressed that the barotropic governor reduces eddy amplitude not by simply increasing the inefficiency of barotropic energy conversion, but by decreasing baroclinic production. Further investigation is needed to better understand these dynamic processes. The inefficiency of barotropic energy conversion is attributable to a change in the eddy structure in the presence of the TP. As the westerly jet strengthens, eddy structure tends to become less efficient

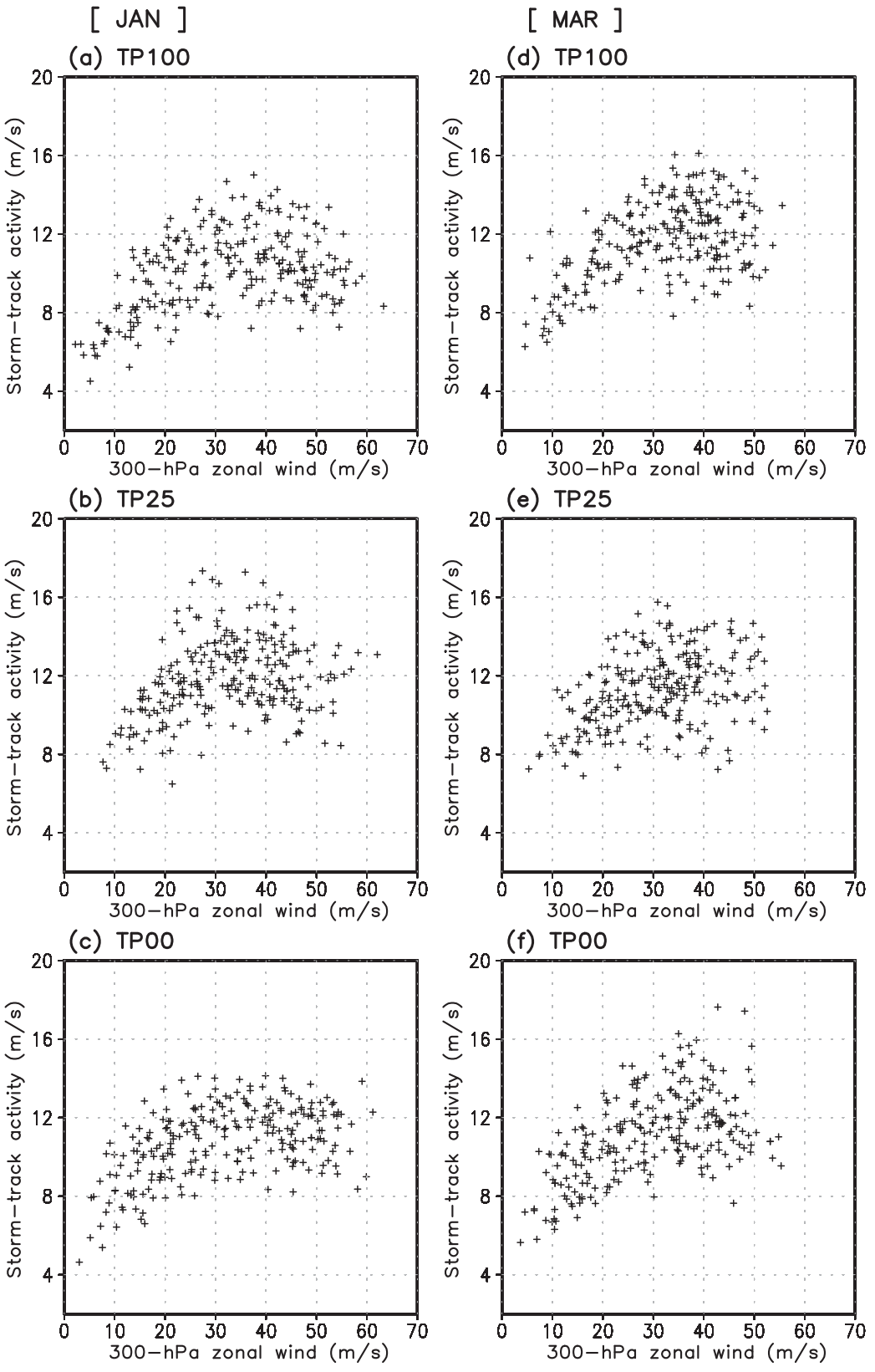

FIG. 10. Scatter diagram of the PST activity and the Pacific jet intensity during (left) January and (right) March in (a),(d) TP100, (b),(e) TP25, and (c),(f) TP00. The storm-track activity and the jet are averaged over (35°–50°N, 140°E–140°W) and (35°–50°N, 120°E–170°W), respectively.

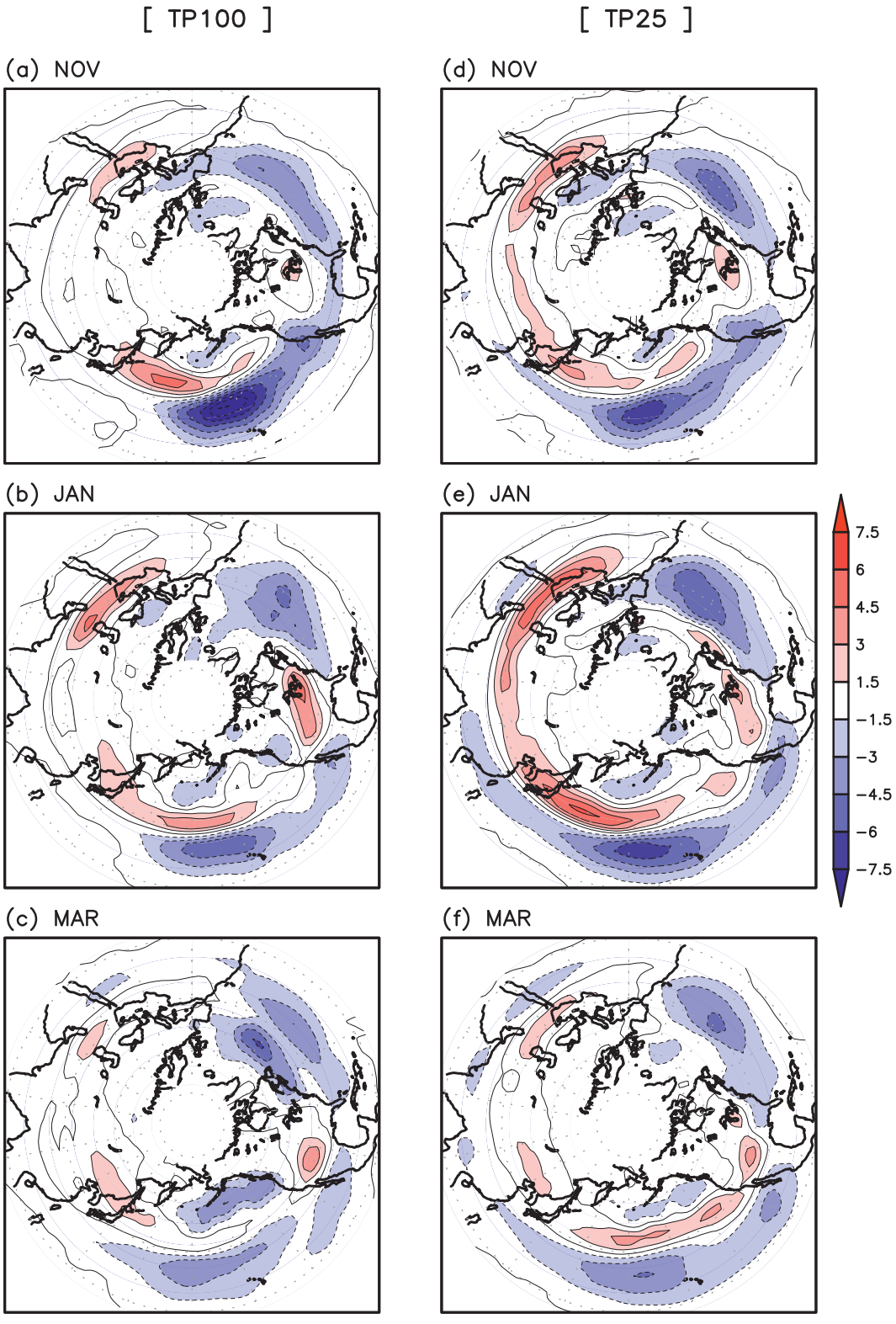

FIG. 11. The kinetic energy conversion (W m^{-2}) at 300 hPa related to the shearing deformation in (a)–(c) TP100 and (d)–(f) TP25 during (top) November, (middle) January, and (bottom) March in the NH.

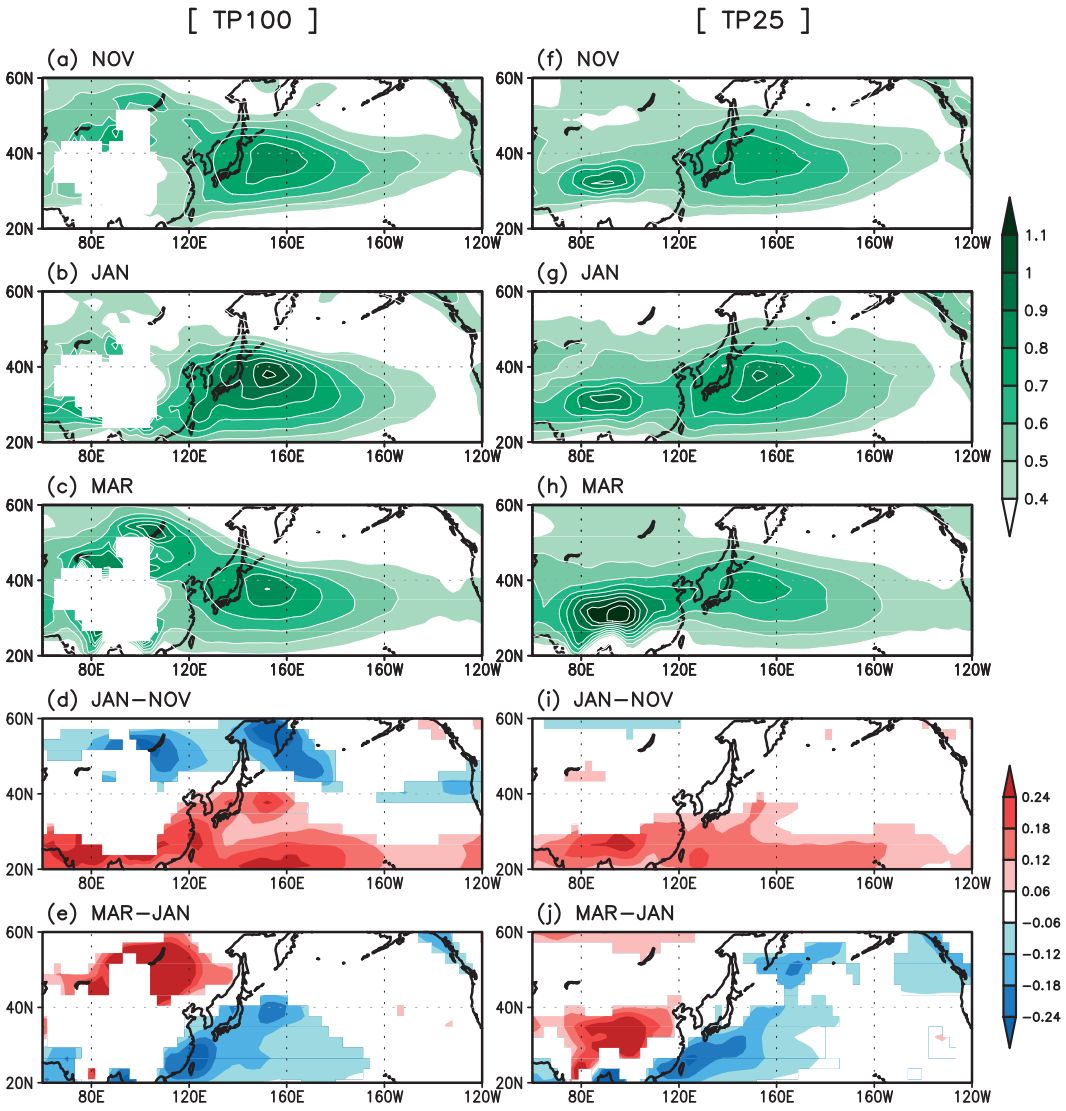

FIG. 12. The 700–850-hPa maximum Eady growth rate (day^{-1}) in (left) TP100 and (right) TP25: (a),(f) November; (b),(g) January; (c),(h) March; (d),(i) difference between January and November; and (e),(j) difference between March and January. Shading in (d),(e),(i),(j) denotes that the differences are significant at a 95% confidence level.

in converting the mean flow energy into eddy energy (Chang 2001; Nakamura et al. 2002). In addition to an inefficient barotropic conversion, a weak baroclinic generation is found during midwinter in TP100 (not shown). It is also shown in the experiments that the eddy structure in TP100 is less anisotropic with a smaller axial tilt over East Asia and the western North Pacific than that in TP25, leading to a weakening of PST activity in January (not shown).

b. *Changes in baroclinicity over the northern part of TP*

Baroclinicity is among the major factors for transient eddy development. The Eady growth rate (Lindzen and Farrell 1980) is used in this study as a measure of baroclinicity in the atmosphere. Since storm-track activity is closely related to the low-level Eady growth rate (e.g., Hoskins and Valdes 1990; Nakamura and Shimpo 2004; Penny et al. 2010; Lee et al. 2011), we compare the 700–850-hPa maximum Eady growth rate in the TP100 and TP25 experiments. Figure 12 presents a 700–850-hPa maximum Eady growth rate in November, January, and March in TP100 and TP25. Over the western North Pacific, the seasonal variation of baroclinicity is similar between the two experiments exhibiting a maximum in January. Differences in baroclinicity between the two experiments, however, are notable over the TP area. In TP100, the baroclinicity over the northern part of the TP is minimum in January but maximum in March. On the other hand, TP25 shows a gradual increase

of baroclinicity from November to March over the southern part of the TP.

The Eady growth rate is dependent on static stability and vertical wind shear. Using reanalysis data, Penny et al. (2010) suggested that the near-surface static stability over the Eurasian continent could exert significant control on the midwinter suppression of PST activity. Based on an atmospheric GCM result, however, Park et al. (2010) addressed that there are minimal changes of near-surface static stability with the TP height. Therefore, we examine changes in static stability and vertical wind shear with the TP height. The annual cycle of baroclinicity and its related components, that is, static stability and vertical wind shear, in TP100 are compared with those in TP25. Area averages over the region (40°–60°N, 80°–120°E) where large differences are found, are used for the comparison. Following Penny et al. (2010), the Eady growth rate can be expressed in terms of static stability and vertical wind shear as follows:

$$\frac{\Delta\sigma}{\overline{\sigma}} \approx \frac{\Delta\lambda}{\overline{\lambda}} - \frac{\Delta N}{\overline{N}},$$

where σ indicates the maximum Eady growth rate, λ represents vertical wind shear, and N is static stability. An overbar denotes the annual mean and Δ implies departure from the annual mean. The temporal evolution of static stability, vertical wind shear, and the Eady growth rate over the northern part of the TP is shown in Fig. 13. There is a distinct seasonality of static stability with a maximum in December or January in a realistic TP height condition, suggesting a strong TP effect on stabilizing the atmosphere. Vertical wind shear shows a minimum in January, which is somewhat different from the observational result in Penny et al. (2010). A strong static stability and a weak wind shear in January results in a minimum Eady growth rate, consequently reducing baroclinicity over the northern part of the TP; this leads to the midwinter suppression of the PST in TP100. In the TP25 experiment, however, static stability does not change much over the northern part of the TP although a maximum is seen in midwinter. Vertical wind shear also exhibits insignificant changes during the cold season. As a result, only a slight decrease in the Eady growth rate is seen between November and January, and hence, baroclinicity cannot contribute in any substantial way to the midwinter suppression of PST activity.

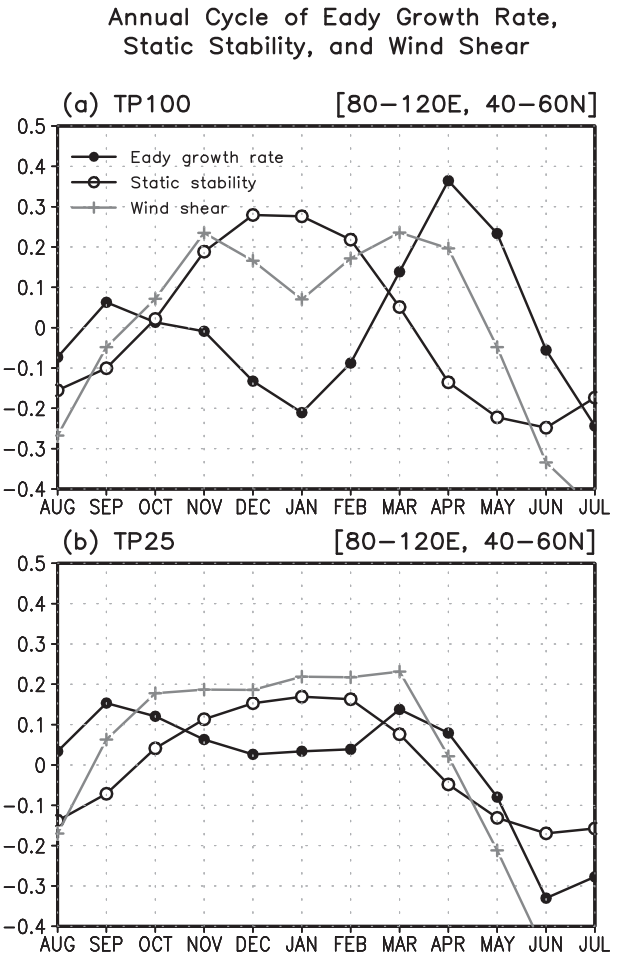

FIG. 13. The annual cycle of near-surface Eady growth rates along with contributions from static stability and wind shear averaged over the region (40°–60°N, 80°–120°E) in the 700–850-hPa layer in (a) TP100 and (b) TP25.

c. *The effect of SST change*

An examination of the effect of SST change, as a result of circulation change in the presence of the TP, on the subseasonal variability of storm-track activity, differences in SST, low-level circulation, and moist static energy between TP100 and TP25 is shown in Fig. 14. It appears that the SST change from the TP contributes to the PST peak in March. Figure 14 indicates that the northerly anomaly from the enhanced Siberian high and the Aleutian low causes a negative SST anomaly over the North Pacific including the coastal seas off the Korean Peninsula and Japan, as discussed in Seager et al. (2002). Kitoh (2002) addressed that an SST decrease to the east of Japan in the CGCM in the present-day orography run is much smaller than that in the atmosphere/mixed layer ocean coupled model, because ocean circulation in the former tends to reduce SST change.

It is noted that the change in the easterly trade winds is significant in the central and western equatorial Pacific in the mountain uplift experiment using the MRI-CGCM (Kitoh 2007). With high mountains, warmer water appears in the western Pacific and eastern Indian Ocean

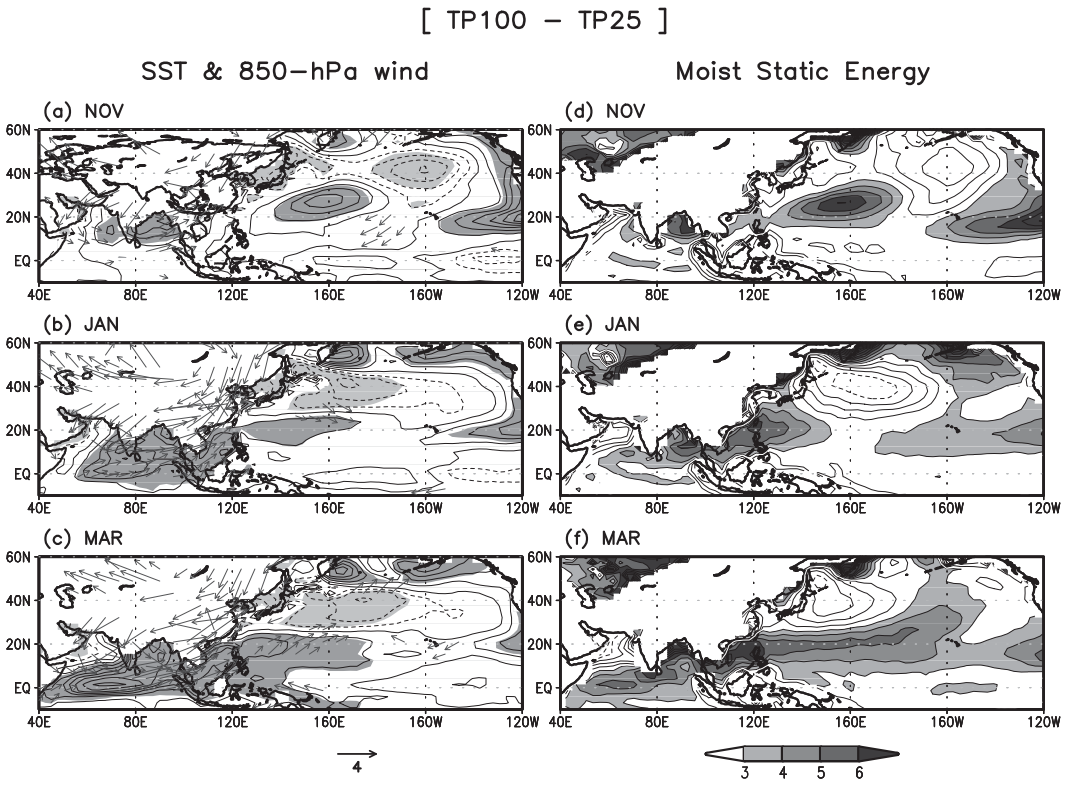

FIG. 14. Difference in (left) SST (contour; K) and 850-hPa wind [vector, reference vector below (c); m s^{-1}], and (right) moist static energy (kJ kg^{-1}) between TP100 and TP25 in (top) November, (middle) January, and (bottom) March. Shading in (a)–(c) indicates that the SST difference is significant at a 95% confidence level. Only vectors significant at a 95% confidence level are shown in (a)–(c).

because of stronger easterly trade winds in the western equatorial Pacific and southwesterly winds in the Indian Ocean, respectively. In our experiment, the TP100-minus-TP25 difference exhibits warm SST anomaly along with anomalous westerly winds in the Indian Ocean and the western equatorial Pacific. The anomalous westerly in the Indian Ocean and the western equatorial Pacific is more prominent in March than in November or January. With an SST increase, particularly in March, moist static energy increases significantly over the entire western Pacific (Fig. 14). The enhanced moist static energy may play some role in strengthening the storm-track activity over the North Pacific, given a weaker baroclinicity over the region in March than in November or January.

6. Summary and discussion

This study investigated the role of the TP on modulating the seasonal mean and the annual variation of atmospheric circulation and transient eddy activity by conducting a numerical experiment with various TP heights using MRI-CGCM 2.3.2. Specific changes in the winter-mean climate, storm-track activity, and its subseasonal variability by the TP are explored.

It is demonstrated that the annual variation of atmospheric circulation and storm-track activities are significantly modulated by the TP. The shape and intensity of zonal wind meandering during the cold season in the upper troposphere over the TP and the Pacific are affected by the presence of the TP. Analysis of stationary eddies reveals that the Siberian high and the Aleutian low are enhanced with the TP, and subsequently strong northwesterly winds along the eastern boundary of the Asian continent strengthen the EAWM in TP100. In the TP25 experiment, however, the circulation pattern over East Asia is characterized by the dominance of zonal wind and northerly wind restricted to the northeastern part of the Asian continent and to the Sea of Okhotsk. This indicates that the TP is responsible for the distinct annual cycle of meridional wind over East Asia. Liu and Yin (2002) showed that there was no significant northerly wind in north China under the ''no topography'' condition and suggested that the influence of the TP is more significant on the EAWM than the summer monsoon.

It is noted that the MRI-CGCM is capable of reproducing the midwinter suppression of PST activity and the double peaks in the annual cycle with a realistic TP.

The midwinter suppression of PST activity becomes less pronounced as the TP height decreases, and thus the TP25 experiment simulates a single peak in the annual cycle with a maximum storm-track activity in midwinter. This implies that the TP plays an important role in generating the midwinter suppression of PST activity. In this study, it is found that the TP tends to modulate the annual cycle of the PST in three different ways. First, the TP tends to modulate the seasonal variation of the Pacific jet, which contributes to the midwinter suppression of PST activity as a barotropic governor. In TP100, the Pacific jet in January is significantly intensified by the TP, and consequently results in a weakening of the PST despite a strong baroclinicity over the Pacific. The destructive effect of an excessively fast jet as a result of the TP is responsible for a structural change of eddies, which lead to an inefficiency of barotropic energy conversion from the mean flow to eddies. Second, the TP tends to modulate the annual cycle of baroclinicity over the northern part of the TP, which contributes to the initiation of the annual cycle of transient eddies. A weak baroclinicity over the northern part of the TP in January in TP100 may lead to a weakening of storm-track activities particularly over the northern part of the TP and East Asia. Third, the considerably warmer SST over the Indian Ocean and the western Pacific with a stronger westerly anomaly in TP100 than in TP25 may enhance moist static energy and contribute to the intensification of the PST in March.

Storm-track activity is linked to several factors such as diabatic heating (Chang 2001) and teleconnection patterns (Nie et al. 2008; Pinto et al. 2011), in addition to the structure of background flow (Nakamura 1992; Nakamura and Sampe 2002; Lee and Kim 2003). Therefore, more studies are needed to examine how the TP alters the effect of these factors on the midwinter minimum of PST activity; such studies may help better understand the subseasonal variability of the storm-track activities.

How the Siberian high, the EAWM, and storm-track activities will be changed under anthropogenic global warming (e.g., Wu et al. 2011; Lee and Wang 2013) is an important question in a climate projection. An investigation under different external forcings, including mountain uplift, should give us good insight into the mechanism and historical/future change of the prominent NH winter climate system.

Acknowledgments. This work was supported by the Global Research Laboratory (GRL) grant of the National Research Foundation (NRF) funded by the Korean Government (Ministry of Education, Science and Technology; 2011-0021927). JYL and BW were supported by the Japan Agency for Marine-Earth Science and Technology (JAMSTEC), NASA (NNX07AG53G), and NOAA (NA17RJ1230) through their sponsorship of research activities at the International Pacific Research Center (IPRC). The authors sincerely thank anonymous reviewers and Professor Kwang-Yul Kim for their valuable comments that helped to improve our manuscript.

REFERENCES

Abe, M., A. Kitoh, and T. Yasunari, 2003: An evolution of the Asian summer monsoon associated with mountain uplift—Simulation with the MRI atmosphere-ocean coupled GCM. *J. Meteor. Soc. Japan,* **81,** 909–933.

——, T. Yasunari, and A. Kitoh, 2004: Effects of large-scale orography on the coupled atmosphere-ocean system in the tropical Indian and Pacific oceans in boreal summer. *J. Meteor. Soc. Japan,* **82,** 745–759.

Branstator, G., 1992: The maintenance of low-frequency atmospheric anomalies. *J. Atmos. Sci.,* **49,** 1924–1945.

Broccoli, A. J., and S. Manabe, 1992: The effects of orography on midlatitude Northern Hemisphere dry climates. *J. Climate,* **5,** 1181–1201.

Chang, E. K. M., 2001: GCM and observational diagnoses of the seasonal and interannual variations of the Pacific storm track during the cool season. *J. Atmos. Sci.,* **58,** 1784–1800.

——, 2009: Diabatic and orographic forcing of northern winter stationary waves and storm tracks. *J. Climate,* **22,** 670–688.

——, and W. Lin, 2011: Comments on ''The role of the central Asian mountains on the midwinter suppression of North Pacific storminess.'' *J. Atmos. Sci.,* **68,** 2800–2803.

Chen, G., I. M. Held, and W. A. Robinson, 2007: Sensitivity of the latitude of the surface westerlies to surface friction. *J. Atmos. Sci.,* **64,** 2899–2915.

Held, I. M., M. Ting, and H. Wang, 2002: Northern winter stationary waves: Theory and modeling. *J. Climate,* **15,** 2125–2144.

Hoskins, B. J., and P. J. Valdes, 1990: On the existence of storm tracks. *J. Atmos. Sci.,* **47,** 1854–1864.

James, I. N., 1987: Suppression of baroclinic instability in horizontally sheared flows. *J. Atmos. Sci.,* **44,** 3710–3720.

Kanamitsu, M., W. Ebisuzaki, J. Woollen, S.-K. Yang, J. J. Hnilo, M. Fiorino, and G. L. Potter, 2002: NCEP—DOE AMIP-II Reanalysis (R-2). *Bull. Amer. Meteor. Soc.,* **83,** 1631–1643.

Kitoh, A., 2002: Effects of large-scale mountains on surface climate: A coupled ocean–atmosphere general circulation model study. *J. Meteor. Soc. Japan,* **80,** 1165–1181.

——, 2004: Effect of mountain uplift on East Asian summer climate investigated by a coupled atmosphere–ocean GCM. *J. Climate,* **17,** 783–802.

——, 2007: ENSO modulation by mountain uplift. *Climate Dyn.,* **28,** 781–796.

Lee, J.-Y., and B. Wang, 2013: Future change of global monsoon in the CMIP5. *Climate Dyn.,* doi:10.1007/s00382-012-1564-0, in press.

——, and Coauthors, 2010: How are seasonal prediction skills related to models' performance on mean state and annual cycle? *Climate Dyn.,* **35,** 267–283.

——, S.-S. Lee, B. Wang, K.-J. Ha, and J.-G. Jhun, 2013: Seasonal prediction and predictability of the Asian winter temperature variability. *Climate Dyn.,* doi:10.1007/s00382-012-1588-5, in press.

Lee, S., and H.-K. Kim, 2003: The dynamical relationship between subtropical and eddy-driven jets. *J. Atmos. Sci.,* **60,** 1490–1503.

Lee, S.-S., J.-Y. Lee, B. Wang, F. F. Jin, W.-J. Lee, and K.-J. Ha, 2011: A comparison of climatological subseasonal variations in the wintertime storm track activity between the North Pacific and Atlantic: Local energetics and moisture effect. *Climate Dyn.,* **37,** 2455–2469.

——, ——, ——, K.-J. Ha, K.-Y. Heo, F.-F. Jin, D. M. Straus, and J. Shukla, 2012: Interdecadal changes in the storm track activity over the North Pacific and North Atlantic. *Climate Dyn.,* **39,** 313–327.

Lee, W.-J., and M. Mak, 1996: The role of orography in the dynamics of storm tracks. *J. Atmos. Sci.,* **53,** 1737–1750.

Lindzen, R. S., and B. Farrell, 1980: A simple approximate result for the maximum growth rate of baroclinic instabilities. *J. Atmos. Sci.,* **37,** 1648–1654.

Liu, X., and Z. Y. Yin, 2002: Sensitivity of East Asian monsoon climate to the uplift of the Tibetan Plateau. *Palaeogeogr., Palaeoclimatol., Palaeoecol.,* **183,** 223–245.

Liu, Y., G. Wu, J. Hong, B. Dong, A. Duan, Q. Bao, and L. Zhou, 2012: Revisiting Asian monsoon formation and change associated with Tibetan Plateau forcing: II. Change. *Climate Dyn.,* **39,** 1183–1195.

Nakamura, H., 1992: Midwinter suppression of baroclinic wave activity in the Pacific. *J. Atmos. Sci.,* **49,** 1629–1642.

——, and T. Sampe, 2002: Trapping of synoptic scale disturbances into the North-Pacific subtropical jet core in midwinter. *Geophys. Res. Lett.,* **29,** 1761, doi:10.1029/2002GL015535.

——, and A. Shimpo, 2004: Seasonal variations in the Southern Hemisphere storm tracks and jet streams as revealed by reanalysis dataset. *J. Climate,* **17,** 1828–1844.

——, T. Izumi, and T. Sampe, 2002: Interannual and decadal modulations recently observed in the Pacific storm-track activity and East Asian winter monsoon. *J. Climate,* **15,** 1855–1874.

Nie, J., P. Wang, W. Yang, and B. Tan, 2008: Northern hemisphere storm tracks in strong AO anomaly winters. *Atmos. Sci. Lett.,* **9,** 153–159.

Park, H.-S., J. C. H. Chiang, and S.-W. Son, 2010: The role of the central Asian mountains on the midwinter suppression of North Pacific storminess. *J. Atmos. Sci.,* **67,** 3706–3720.

——, ——, and ——, 2011: Reply. *J. Atmos. Sci.,* **68,** 2804–2806.

Penny, S., G. H. Roe, and D. S. Battisti, 2010: The source of the midwinter suppression in storminess over the North Pacific. *J. Climate,* **23,** 634–648.

Pinto, J. G., M. Reyers, and U. Ulbrich, 2011: The variable link between PNA and NAO in observations and in multi-century CGCM simulations. *Climate Dyn.,* **36,** 337–354.

Saulière, J., D. J. Brayshaw, B. Hoskins, and M. Blackburn, 2012: Further investigation of the impact of idealized continents and SST distributions on the Northern Hemisphere storm tracks. *J. Atmos. Sci.,* **69,** 840–856.

Seager, R., D. S. Battisti, J. Yin, N. Gordon, N. Naik, A. C. Clement, and M. A. Cane, 2002: Is the Gulf Stream responsible for Europe's mild winters? *Quart. J. Roy. Meteor. Soc.,* **128,** 2563–2586.

Son, S.-W., M. Ting, and L. M. Polvani, 2009: The effect of topography on storm-track intensity in a relatively simple general circulation model. *J. Atmos. Sci.,* **66,** 393–411.

Wang, B., Z. Wu, C. P. Chang, J. Liu, and T. Zhou, 2010: Another look at interannual-to-interdecadal variations of the East Asian winter monsoon: The northern and southern temperature modes. *J. Climate,* **23,** 1495–1512.

Wu, G., and Coauthors, 2007: The influence of mechanical and thermal forcing by the Tibetan Plateau on Asian climate. *J. Hydrometeor.,* **8,** 770–789.

——, Y. Liu, B. Dong, X. Liang, A. Duan, Q. Bao, and J. Yu, 2012a: Revisiting Asian monsoon formation and change associated with Tibetan Plateau forcing: I. Formation. *Climate Dyn.,* **39,** 1169–1181.

——, ——, B. He, Q. Bao, A. Duan, and F.-F. Jin, 2012b: Thermal controls on the Asian summer monsoon. *Sci. Rep.,* **2,** 404, doi:10.1038/srep00404.

Wu, Y., M. Ting, R. Seager, H.-P. Huang, and M. A. Cane, 2011: Changes in storm tracks and energy transports in a warmer climate simulated by the GFDL CM2.1 model. *Climate Dyn.,* **37,** 53–72.

Yukimoto, S., and Coauthors, 2001: The new Meteorological Research Institute coupled GCM (MRI-CGCM2)—Model climate and variability. *Pap. Meteor. Geophys.,* **51,** 47–88.

——, A. Noda, T. Uchiyama, S. Kusunoki, and A. Kitoh, 2006: Climate changes of the twentieth through twenty-first centuries simulated by the MRI-CGCM2.3. *Pap. Meteor. Geophys.,* **56,** 9–24.